Distinctive membrane and discharge properties of rat spinal lamina I projection neurones *in vitro*

Ruth Ruscheweyh, Hiroshi Ikeda, Bernhard Heinke and Jürgen Sandkühler

Brain Research Institute, Medical University of Vienna, Vienna, Austria

Most lamina I neurones with a projection to the brainstem express the neurokinin 1 receptor and thus belong to a small subgroup of lamina I neurones that are necessary for the development of hyperalgesia in rat models of persisting pain. These neurones are prone to synaptic plasticity following primary afferent stimulation in the noxious range while other nociceptive lamina I neurones are not. Here, we used whole-cell patch-clamp recordings from lamina I neurones in young rat spinal cord transverse slices to test if projection neurones possess membrane properties that set them apart from other lamina I neurones. Neurones with a projection to the parabrachial area or the periaqueductal grey (PAG) were identified by retrograde labelling with the fluorescent tracer DiI. The properties of lamina I projection neurones were found to be fundamentally different from those of unidentified, presumably propriospinal lamina I neurones. Two firing patterns, the gap and the bursting firing pattern, occurred almost exclusively in projection neurones. Most spino-parabrachial neurones showed the gap firing pattern while the bursting firing pattern was characteristic of spino-PAG neurones. The underlying membrane currents had the properties of an A-type K^+ current and a Ca^{2+} curent with a low activation threshold, respectively. Projection neurones, especially those of the burst firing type, were more easily excitable than unidentified neurones and received a larger proportion of monosynaptic input from primary afferent C-fibres. Intracellular labelling with Lucifer yellow showed that projection neurones had larger somata than unidentified neurones and many had a considerable extension in the mediolateral plane.

(Received 26 August 2003; accepted after revision 19 December 2003; first published online 23 December 2003)
Corresponding author J. Sandkühler: Brain Research Institute, Department of Neurophysiology, Medical University of Vienna, Spitalgasse 4, A-1090 Vienna, Austria. Email: juergen.sandkuehler@meduniwien.ac.at

Lamina I of the spinal dorsal horn contains mainly nociceptive neurones (Christensen & Perl, 1970; Cervero & Tattersall, 1987) and is densely innervated by primary afferent Aδ- and C-fibres, many of which are nociceptive (Willis & Coggeshall, 1991). In the rat, 5–10% of the lamina I neurones send projections to the brain (Bice & Beal, 1997*a*,*b*; Spike *et al.* 2003), thus relaying primary afferent information directly to nociceptive centres like the thalamus, the parabrachial area and the periaqueductal grey (PAG) (Marshall *et al.* 1996; Todd *et al.* 2000). There, discriminative evaluation of the painful stimuli takes place and autonomic and emotional responses and pain-related behaviour are generated (Bester *et al.* 2000; Gauriau & Bernard, 2002; Keay & Bandler, 2002). In addition, recent evidence indicates that lamina I projection neurones may have a decisive role in the development and maintenance of persisting pain. In the rat, the group of lamina I projection neurones seems to largely overlap the subset of lamina I neurones that express the NK1 receptor (Ding *et al.* 1995; Todd *et al.* 2000). Selective destruction of the NK1 receptor-expressing lamina I neurones by intrathecal application of the cytotoxin saporin conjugated to substance P strongly attenuates hyperalgesia, allodynia and central sensitization in rat models of inflammatory and neuropathic pain but leaves responses to acute, mildly painful stimuli unaffected (Mantyh *et al.* 1997; Nichols *et al.* 1999; Khasabov *et al.* 2002; Suzuki *et al.* 2002). Information on the properties of lamina I projection neurones is therefore important to understand how they code nociceptive information for transmission to the brain and how they contribute to central sensitization and persisting pain. Retrograde labelling from supraspinal targets allows identification of these neurones in a spinal slice preparation and selective recording of them with the patch-clamp technique (Ikeda *et al.* 2003). Using this approach, we have recently shown that in lamina I neurones with a projection to the parabrachial area or the PAG, conditioning stimulation of C-fibre input from

 DOI: 10.1113/jphysiol.2003.054049

the dorsal root induces synaptic long-term potentiation (Ikeda *et al.* 2003; and authors' unpublished observations), which is a cellular model of centrally mediated hyperalgesia (Sandkühler, 2000). C-fibre synapses with unidentified lamina I neurones were, in contrast, not potentiated. Here, we have analysed membrane and discharge properties and types of afferent input in spino-parabrachial and spino-PAG neurones in lamina I and compared them to the properties of unidentified neurones.

Methods

Retrograde labelling of spino-parabrachial and spino-PAG neurones

Stereotaxic injections were performed as previously described (Ikeda *et al.* 2003). Briefly, 18- to 23-day-old Sprague-Dawley rats were anaesthetized with a mixture of ketamine and xylazine (75 mg kg^{-1} and 7.5 mg kg^{-1} I.P.) and placed in a stereotaxic apparatus. A small (< 1 cm) scalp cut was made and a hole was drilled into the skull bone over the targeted injection area. A 500 nl Hamilton syringe was used to inject 50–100 nl of DiI (1.25–2.5%) into the right lateral parabrachial area or into the right caudal and/or intermediate ventrolateral and lateral PAG. The head wound was closed with two stitches and inspected daily. No signs of infection were detected. After recovery from the anaesthesia, the animals fed and drank normally. No pain-related behaviour was observed in any of the animals. After a 2–4-day survival period, spinal cord slices were prepared as described below. The brain was removed, cooled to -20°C in isopentane and cryostat sections (30 μm thick) of the brainstem were obtained to allow histological verification of the injection site (Fig. 1*A* and *B*). Only recordings from animals where the injection site clearly involved either the parabrachial area or the PAG but not both were included in the present study.

Preparation of spinal cord slices

The lumbar spinal cord was removed from 20- to 26-day-old Sprague-Dawley rats under deep ether anaesthesia. The rats were then killed by an overdose of ether. Transverse slices, 500 μm thick, most of them with an attached dorsal root (6–12 mm long), were cut on a microslicer (DTK-1000, Dosaka, Kyoto, Japan). Slices were stored in an incubation solution (mM: NaCl 95, KCl 1.8, KH_2PO_4 1.2, $CaCl_2$ 0.5, $MgSO_4$ 7, $NaHCO_3$ 26, glucose 15, sucrose 50, oxygenated with 95% O_2, 5% CO_2; pH 7.4, measured osmolality 310–320 mosmol kg^{-1}). For recording, a single slice was transferred to the recording chamber where it was superfused by recording solution at 3 ml min^{-1} at room temperature (20–24°C). The recording solution was identical to the incubation solution except for (mM): NaCl 127, $CaCl_2$ 2.4, $MgSO_4$ 1.3 and sucrose 0. All procedures used conformed to the guidelines of the Austrian Federal Ministry for Education, Science and Culture.

Patch-clamp recording

Dorsal horn neurones were visualized with Dodt-infrared optics. Retrogradely labelled spino-parabrachial and spino-PAG neurones in lamina I detected by epifluorescence and unidentified (not labelled) lamina I neurones were recorded in the whole-cell patch-clamp configuration with glass pipettes (2–6 MΩ) filled with internal solution (mM: potassium gluconate 120, KCl 20, $MgCl_2$ 2, Na_2ATP 2, NaGTP 0.5, Hepes 20, EGTA 0.5, pH 7.28 with KOH, measured osmolality 300 mosmol kg^{-1}) as described elsewhere (Ruscheweyh & Sandkühler, 2002). Voltage- and current-clamp recordings were made using an Axopatch 200B amplifier and the pCLAMP 8 or 9 acquisition software (Axon Instruments). Signals were low-pass filtered at 2–5 kHz, amplified 5-fold, sampled at 5–10 kHz and analysed offline using pCLAMP 9. Series resistance was usually between 5 and 25 MΩ. No correction for the liquid junction potential was made. The mediolateral location of the recorded lamina I neurone was assessed at the end of the experiment by visually inspecting the position of the pipette tip under a 4 × objective.

Passive membrane properties

The membrane potential measured immediately after establishing the whole-cell configuration was called the 'resting membrane potential' even though the membrane potential of a neurone in a slice preparation superfused by artificial cerebrospinal fluid and measured in the whole-cell configuration is probably not equivalent to the situation in the intact animal. Only neurones that had a resting membrane potential more negative than −50 mV were investigated further. Membrane resistance and capacitance were calculated from the reaction to 100 ms-long hyperpolarizing voltage steps from −70 to −80 mV. The responses to 20 such voltage steps were averaged and the membrane resistance was then calculated from the difference in steady-state current at the two voltages. The total membrane capacitance was calculated from the area under the capacitive transient, corresponding to the charge moved by the voltage step. The built-in pCLAMP membrane test was found to be

rather unreliable in determining the membrane resistance, especially for the large projection neurones where the capacitive transient often decayed with several time constants. In general, membrane resistances estimated with the pCLAMP membrane test were too low by a factor of 2–3 even for the smaller unidentified lamina I neurones. This accounts for the difference between the currently (Table 2) and previously (Ruscheweyh & Sandkühler, 2002) reported membrane resistances of unidentified lamina I neurones. In contrast, in small, compact neurones or the pCLAMP model cell, both methods give the same results.

Firing patterns and active membrane properties

Firing patterns were determined in response to depolarizing (usually 25–350 pA in 25 pA steps) current injections of 1 s duration. Firing patterns were routinely elicited from different holding potentials (at least one from between −50 and −65 mV, one from between −65 and −80 mV and one from a potential more negative than −80 mV) to detect voltage dependence of the firing patterns. Voltage-clamp recordings from different holding potentials were used to investigate the underlying currents. The action potential threshold as reported here was measured by means of a voltage step protocol. Holding potential was −80 mV and increasing voltage injections (usually −60 to −30 mV at 2 mV steps, modified if the action potential threshold did not fall into this range) were used to determine the threshold of the fast Na^+ current. This method has the advantage of taking into account the facilitating or inhibiting effect of other voltage-dependent membrane currents like the A- and T-currents reported here on the action potential generation.

The action potential width was determined at the base of the first action potential evoked by depolarizing current injected to determine the firing pattern from a holding potential around −80 mV. The afterdepolarization amplitude was determined from the same action potential, measuring from the point of maximal afterhyperpolarization to the point of maximal afterdepolarization.

Primary afferent stimulation

The dorsal root was stimulated through a suction electrode with a constant current stimulator (WPI, Sarasota) at 0.1 ms pulse width. Excitatory postsynaptic currents (EPSCs) were classified according to their latency and threshold to be Aδ- or C-fibre-evoked as previously described (Chen & Sandkühler, 2000; Ruscheweyh & Sandkühler, 2002). Constant latencies and absence of failures during 10 Hz stimulation (for Aδ-fibres) or 1 Hz stimulation (for C-fibres) were used as criteria for apparently monosynaptic transmission.

Intracellular labelling with Lucifer yellow

In a separate set of experiments, we included Lucifer yellow (0.1%) in the patch pipette solution and filled lamina I unidentified and projection neurones for about 10–20 min. This was not routinely done because we could not exclude the possibility that Lucifer yellow might alter the membrane properties of the recorded neurones (Higure *et al.* 2003). At the end of the recording, the patch pipette was carefully withdrawn from the recorded neurone and the slice was stored in 4% paraformaldehyde in phosphate buffer. For analysis, the slice was cleared in DMSO and inspected under a fluorescence microscope equipped with a CCD camera (Olympus DP50). Two-dimensional reconstructions of the filled neurones in the transverse plane were made using the analySIS Software (Olympus). The same software was used to measure the somatic area and the length of the dendritic tree (sum of all visible dendrites). The mediolateral and dorsoventral extent of the dendritic tree were measured according to the method of Lima and Coimbra (Lima & Coimbra, 1986; Galhardo & Lima, 1999). For neurones lying in the medial two thirds of lamina I, the mediolateral axis was defined to be parallel to the dorsal horn surface while for neurones lying in the lateral third of lamina I, the mediolateral axis was taken to be the tangent to the dorsal horn surface at the location of the neurone. The dorsoventral axis was perpendicular to the mediolateral axis. In some neurones, very long, uniformly thin, seldom-branching processes were seen that probably correspond to axons. These processes were not included in the measurements of the dendritic tree.

Statistical analysis

All values are means ± S.E.M. One-way ANOVA, the non-parametric Mann-Whitney rank-sum test, Student's unpaired *t* test, Fisher's exact test and the χ^2 test were used for statistical comparisons where appropriate. ANOVA was followed by a Mann-Whitney test or a *t* test corrected by the Bonferroni adjustment.

Drugs

Drugs and their sources were as follows: 4-aminopyridine (4-AP, 0.5–5 mM), tetraethylammonium (TEA,

Table 1. Morphometric analysis of lamina I unidentified and projection neurones

	Unidentified neurones (UN) ($n = 11$–12)	Spino-parabrachial neurones (PB) ($n = 8$)	Spino-PAG neurones (PAG) ($n = 9$–10)	ANOVA
Area of cell soma (μm^2)	154 ± 14 **PB, PAG	370 ± 38 **UN	375 ± 64 **UN	$P < 0.001$
Length of dendritic tree (μm)	731 ± 29 *PB	1383 ± 168 *UN	820 ± 188	$P = 0.023$
Mediolateral extent of dendritic tree (μm)	143 ± 22 **PB, *PAG	410 ± 35 **UN	307 ± 45 *UN	$P < 0.001$
Dorsoventral extent of dendritic tree (μm)	187 ± 18	197 ± 28	133 ± 26	$P = 0.138$

Morphometric analysis of the neurones was performed on projections in the transverse plane. Statistical significance was assessed by one-way ANOVA. $^*P < 0.05$, $^{**}P < 0.01$ in the *post hoc* test, followed by the abbreviation of the group the comparison was made with. *n*, number of observations.

20–30 mM) and nickel cloride (Ni^{2+}, 100 μM) were from Sigma (Deisenhofen, Germany), cadmium chloride (Cd^{2+}, 200 μM) from Merck (Hohenbrunn, Germany), tetrodotoxin (TTX, 0.5 μM) from Tocris (Bristol, UK), Lucifer yellow CH dipotassium salt from Fluka (Buchs, Switzerland), and 1,1′-didodecyl-3,3,3′,3′,-tetramethylindocarbocyanine perchlorate ($DiIC_{12}(3)$, DiI, 1.25–2.5%) from Molecular Probes (Leiden, The Netherlands). Stock solutions were prepared by dissolving the drugs in acidic buffer (pH 4.8, tetrodotoxin) or distilled water (4-AP, Cd^{2+}, Ni^{2+}) and stored in aliquots at −20°C. Drugs were added to the superfusion solution at defined concentrations as indicated. DiI was dissolved in DMSO to its final concentration and stored at 4°C. Lucifer yellow was freshly dissolved in pipette solution to a concentration of 0.1% where indicated.

Results

Injection of the retrograde tracer DiI into the parabrachial area or the PAG (Fig. 1*A* and *B*) resulted in predominantly contralateral labelling of lamina I neurones after 2–4 days. Injections into the parabrachial area yielded labelled neurones that were evenly distributed over the mediolateral extent of lamina I. Injections into the PAG stained a smaller number of neurones that were concentrated under the dorsal root entry zone. In addition to fibres terminating in the injected area, some fibres of passage ascending to more rostral structures may also have taken up the dye. The extent of this problem is currently not known. Here, we called neurones retrogradely labelled from the respective areas spino-parabrachial and spino-PAG neurones even though some of them might have had projections to other regions of the brain. Whole-cell patch-clamp recordings were obtained from 301 lamina I neurones which had a projection to the contra- or ipsilateral parabrachial area or PAG or which were unidentified with respect to axonal projection. Thirty lamina I neurones were filled with Lucifer yellow (see Fig. 1*C* for examples) and reconstructed in the transverse plane. Somatic areas of projection neurones were found to be significantly larger than those of unidentified neurones, and spinoparabrachial neurones also had larger dendritic trees than unidentified neurones (Table 1). Many projection neurones had long mediolateral dendrites while the unidentified neurones often had more ventrally orientated dendritic trees (see Fig. 1*C* for examples). This was confirmed by the morphometric data showing that projection neurones had a significantly larger mediolateral extension than unidentified neurones while dorsoventral extents were similar (Table 1). In 17% of the 12 unidentified neurones and in 61% of the 18 projection neurones, a long, uniformly thin, seldom-branching process without spines was seen, which was supposed to be an axon. In projection neurones, these axons typically coursed laterally in lamina I or the overlying white matter, often reaching the lateral edge of the dorsal horn (Fig. 1*C*). Three of the 18 projection neurones filled with Lucifer yellow lay ipsilateral to the injection site. Two of them also had laterally coursing axons which, however, appeared to be much shorter than the average.

Firing patterns

Apart from the five firing patterns (tonic, delayed, initial bursting, single spike, phasic bursting) that we have previously described in unidentified lamina I neurones (Ruscheweyh & Sandkühler, 2002) and that are not illustrated here, two additional firing patterns were identified. The gap firing pattern showed a long first interspike interval, followed by tonic firing. For just suprathreshold current injections, a long delay to the generation of the first action potential occurred (Fig. 2*A*). This firing pattern could be evoked only from holding potentials more negative than about −75 mV (Fig. 9*A* and *B*). The bursting firing pattern was characterized by a short burst of two to four action potentials riding on a slow depolarizing wave at the onset of a depolarizing

current pulse. With stronger current injections, it was followed by tonic firing (Fig. 2*B*). This firing pattern was evident only if the neurone was held at a potential more negative than about −60 mV (Fig. 10*A*). From less negative holding potentials, rebound action potentials were evoked by release from hyperpolarizing current (not shown). These two novel firing patterns were typical of projection neurones (Fig. 3). Seventy-five per cent of the 84 spino-parabrachial neurones showed the gap firing pattern. Most of the 82 spino-PAG neurones exhibited either the gap or the bursting firing pattern. Both were almost absent from the population of unidentified neurones that showed a distribution of firing patterns comparable to our earlier findings (Fig. 3 and Ruscheweyh & Sandkühler, 2002). Three of the spino-PAG neurones showed a bursting firing pattern from a holding potential of about −70 mV and a gap firing pattern from about −85 mV and were grouped among the bursting neurones. No correlation was found between the mediolateral location of the neurones and their firing pattern (not shown).

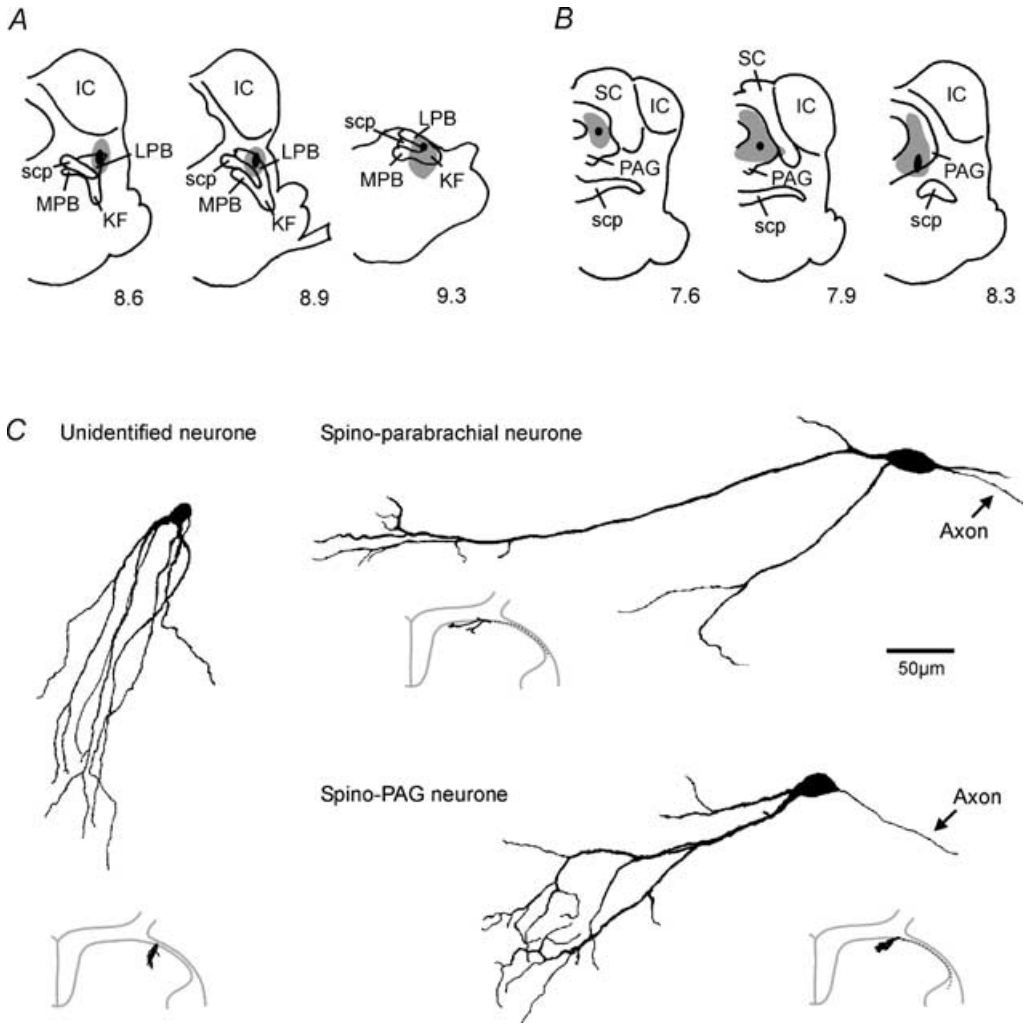

Figure 1. Retrograde labelling of spinal lamina I neurones from the brainstem and morphology of lamina I unidentified and projection neurones

A and *B,* distribution of the fluorescent tracer DiI in the parabrachial area and in the PAG, respectively, in two representative animals 3 days after injection of the dye. Black indicates the areas damaged by the injection; grey indicates the spread of the tracer. IC, inferior colliculus; KF, Kölliker-Fuse nucleus; LPB, lateral parabrachial area; MPB, medial parabrachial area; PAG, periaqueductal grey; SC, superior colliculus; scp, superior cerebellar peduncle. The numbers below each section indicate the distance in millimetres caudal to bregma according to the atlas of L. W. Swanson (1992). *C*, examples of the morphology of lamina I unidentified and projection neurones. Lucifer yellow-filled neurones were reconstructed in the transverse plane. Insets show the position of the neurones in an outline of one dorsal quadrant of the slice. Broken lines in the insets are axons.

The proportion of bursting and gap firing neurones in spino-PAG neurones was dependent on the rostrocaudal position of the injection of the retrograde tracer (Fig. 4). More caudal injection sites revealed a greater number of bursting neurones while more rostral injections preferentially yielded gap firing neurones ($P < 0.01$ for the comparison of the percentages of gap and burst firing neurones at 7.9 and at 8.6 mm caudal to bregma). Two animals had the main injection site more rostrally than those shown in Fig. 4, at 7.6 mm caudal to bregma, and they had equal amounts of bursting and gap firing neurones ($33 \pm 0\%$ each).

Two different A-currents are responsible for the gap and the delayed firing pattern

Delayed firing is the second to third most frequent pattern in unidentified lamina I neurones (Fig. 3 and Ruscheweyh & Sandkühler, 2002). It is similar to the gap firing pattern encountered in projection neurones in that both displayed a voltage-dependent delay in action potential firing in response to a depolarizing current injection. In delayed firing neurones, the delay occurred before the first action potential while in gap firing neurones the delay was reflected by a long first interspike interval (Fig. 5). A voltage-dependent, rapidly activating and inactivating potassium current called A-current is responsible for the delayed firing pattern (Ruscheweyh & Sandkühler, 2002). Voltage-clamp analysis showed that gap firing neurones also exhibited an A-current. It will be called slow A-current because it had noticeably slower kinetics than the fast A-current belonging to the delayed firing pattern. Comparison of the two A-currents showed significant differences in voltage dependence, kinetics and pharmacology. Voltage-dependent activation curves were similar but removal of steady-state inactivation required significantly more negative holding potentials in the slow A-current than in the fast A-current (Fig. 6). This fits with the observation that the gap firing pattern could only be evoked from holding potentials more negative than about −75 mV (Fig. 9*A* and *B*) while a potential more negative that −60 mV usually was sufficient for the delayed firing pattern (not shown, see also Ruscheweyh & Sandkühler, 2002). Superposition of the two currents illustrates the difference in kinetics (Fig. 7*A*). Both the time to peak and the time constant of decay were voltage-dependent and significantly slower in the slow A-current than in the fast A-current (Fig. 7*A* and *B*, $n = 5$, $P < 0.01$). Recovery from inactivation was also significantly slower in the slow A-current (43 ± 8 ms, $n = 6$) than in the fast A-current

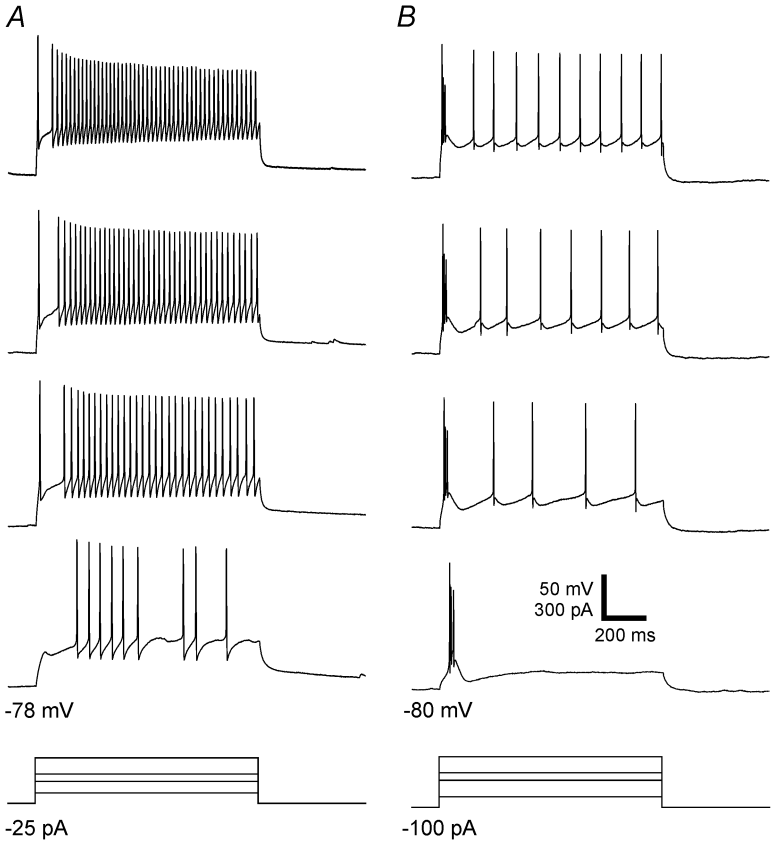

Figure 2. Firing patterns typical of lamina I projection neurones
Firing patterns were obtained in response to depolarizing current injected from hyperpolarized holding potentials. *A*, gap firing pattern, found in most spino-parabrachial neurones. *B*, bursting firing pattern, typical of spino-PAG neurones. Bottom traces: injected currents, superimposed.

(14 ± 2 ms, $n = 6$, $P < 0.01$, Fig. 8). Sensitivity to 4-AP was different in the two currents. 4-AP at 5 mM completely blocked the slow A-current but only partially blocked the fast A-current (to 21 ± 7% of control, $n = 5$, measured at a voltage step from −100−0 mV, Fig. 6*A* and *B*). At a lower concentration (0.5 mM), 4-AP does not affect the fast A-current (Ruscheweyh & Sandkühler, 2002) but it reduced the slow A-current to approximately 50% of control ($n = 4$, not shown). Consistent with this pharmacology, 4-AP (2–5 mM) abolished the gap in gap firing neurones ($n = 5$, Fig. 9*C*).

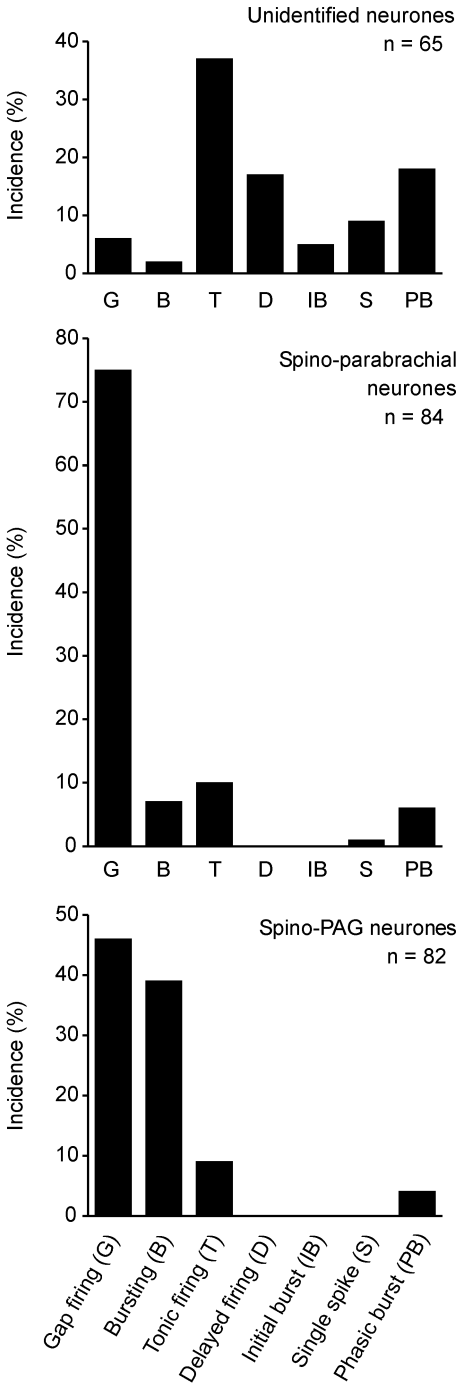

Figure 3. Differential distribution of firing patterns among projection neurones and unidentified neurones in lamina I
Percentages of neurones showing the respective firing pattern are given. One per cent of the spino-parabrachial neurones and two per cent of the spino-PAG neurones could not be classified as belonging to any of these firing patterns and were omitted from the figure.

Properties of the bursting firing pattern

The bursting firing pattern was voltage-dependent, converting into a tonic firing pattern, albeit often with

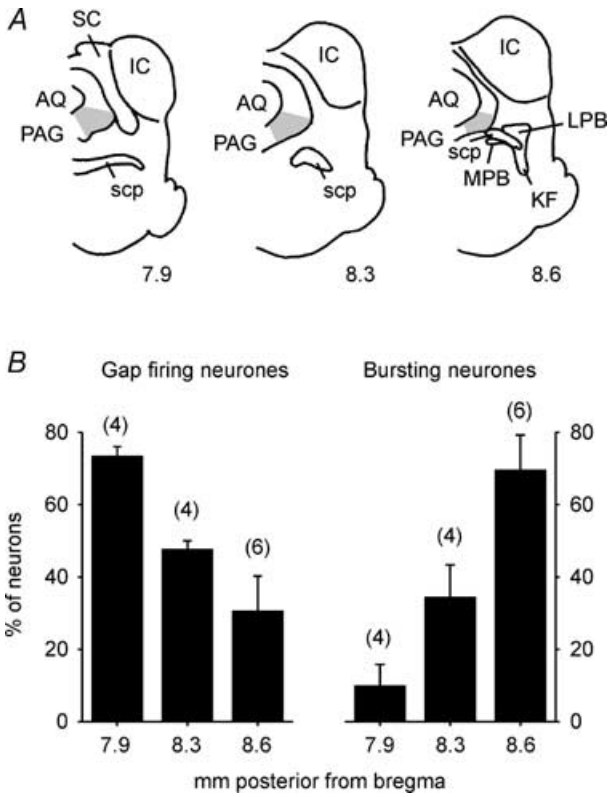

Figure 4. The proportion of gap firing to burst firing spino-PAG neurones depends on the rostrocaudal location of the tracer injection
Animals were grouped according to the level caudal to bregma where the greatest amount of tracer in the ventrolateral PAG was found. When that was equally true for two levels, the animal was classified as belonging to the more caudal level. *A* shows sections of the three rostrocaudal levels to which 14 of the 16 animals with injections in the PAG included in the present study could be grouped. The shaded areas indicate the location of the ventrolateral PAG at the respective levels. AQ, aqueduct; other abbreviations are as in Fig. 1. The numbers below each section indicate the distance in millimetres caudal to bregma according to the atlas of Swanson (1992). *B,* the percentages of neurones showing the gap or bursting firing pattern were determined for each animal, and mean ± S.E.M. values are shown. Numbers of animals in each group are given in parentheses.

a strong frequency adaptation, when the neurone was held at a potential more depolarized than about −60 mV (n = 10, Fig. 10*A*). Block of the action potentials with TTX (0.5 μM) in burst firing neurones revealed a transient depolarizing wave in response to the current injection (n = 11, Fig. 10*B*). The corresponding transient inward current could be seen in voltage-clamp recordings and activated well below the action potential threshold (−60 ± 2 mV, n = 4, not shown). This current was not affected by TTX but was partially blocked by Ni^{2+} (100 μM, n = 4, not shown, block to ∼50% of control) and Cd^{2+} (200 μM, n = 2, not shown, block to 10 and 50% of control), suggesting that it was a Ca^{2+} current. We did not further investigate this presumably low-threshold Ca^{2+} current because we did not find a combination of Ca^{2+} channel antagonists that reliably blocked the Ca^{2+} currents activating at higher voltages without affecting the low-threshold current described here.

Active and passive membrane properties

Lamina I neurones with different brainstem projections showed prominent differences in the shape of action potentials and their afterpotentials. Unidentified neurones had either a monophasic (Fig. 11*A*) or a polyphasic afterhyperpolarization as previously described (Ruscheweyh & Sandkühler, 2002). Seventy-eight per cent of the 96 spino-parabrachial neurones tested exhibited a hump in the falling phase of the action potential (Fig. 11*B*), leading to an increased action potential width compared to the other groups of neurones (Table 2 and Ikeda *et al.* 2003). No correlation between the presence of a hump and a specific firing pattern was found among the spino-parabrachial neurones. Humps in the falling phase of the action potential were not seen in unidentified neurones. Nineteen per cent of the 83 spino-PAG neurones tested showed a hump but none of the 29 burst firing spino-PAG neurones did. Spino-PAG neurones, however, often showed a prominent afterdepolarization following an action potential (Fig. 11*C*). Afterdepolarizations in spino-parabrachial neurones and unidentified neurones were rare and, if present, much smaller in amplitude (Table 2).

Spino-PAG neurones exhibited a less negative resting membrane potential than neurones from the other two groups (Table 2). Due to relatively negative action potential thresholds, the membranes of projection neurones were more easily excitable than those of unidentified neurones,

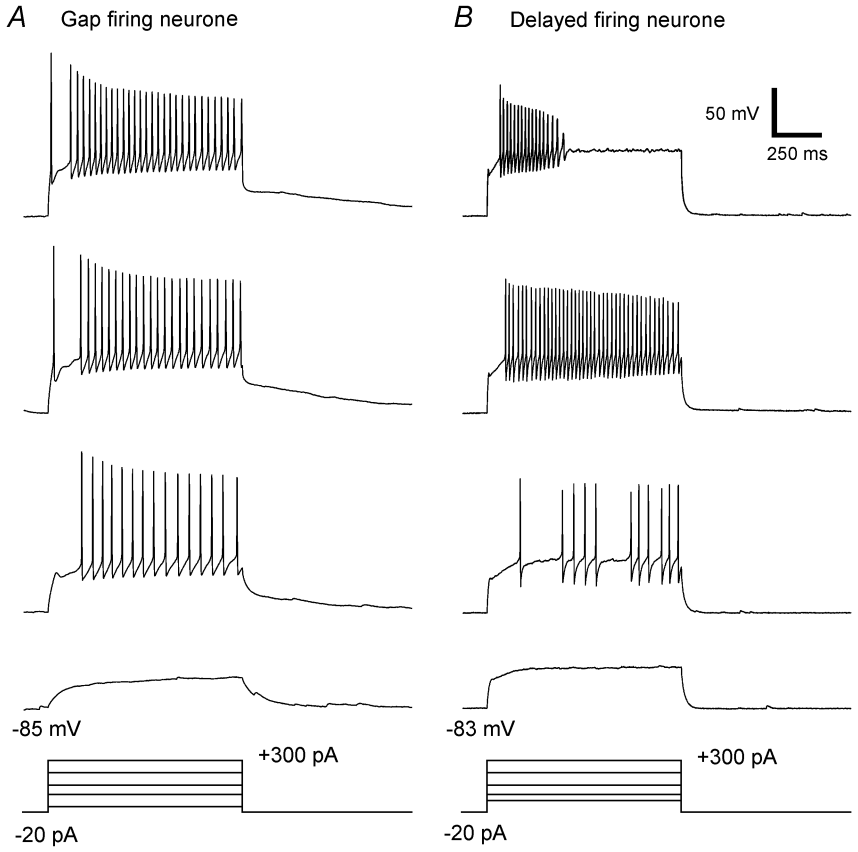

Figure 5. Comparison of the gap and the delayed firing pattern
A and *B,* representative examples of a gap and a delayed firing neurone, respectively. Note that in both firing patterns there is a slow ramp depolarization in response to subthreshold current pulses. Both the long first interspike interval in the gap firing neurone and the delay to the first action potential in the delayed firing neurone shorten with stronger current injections. Bottom traces: injected currents, superimposed.

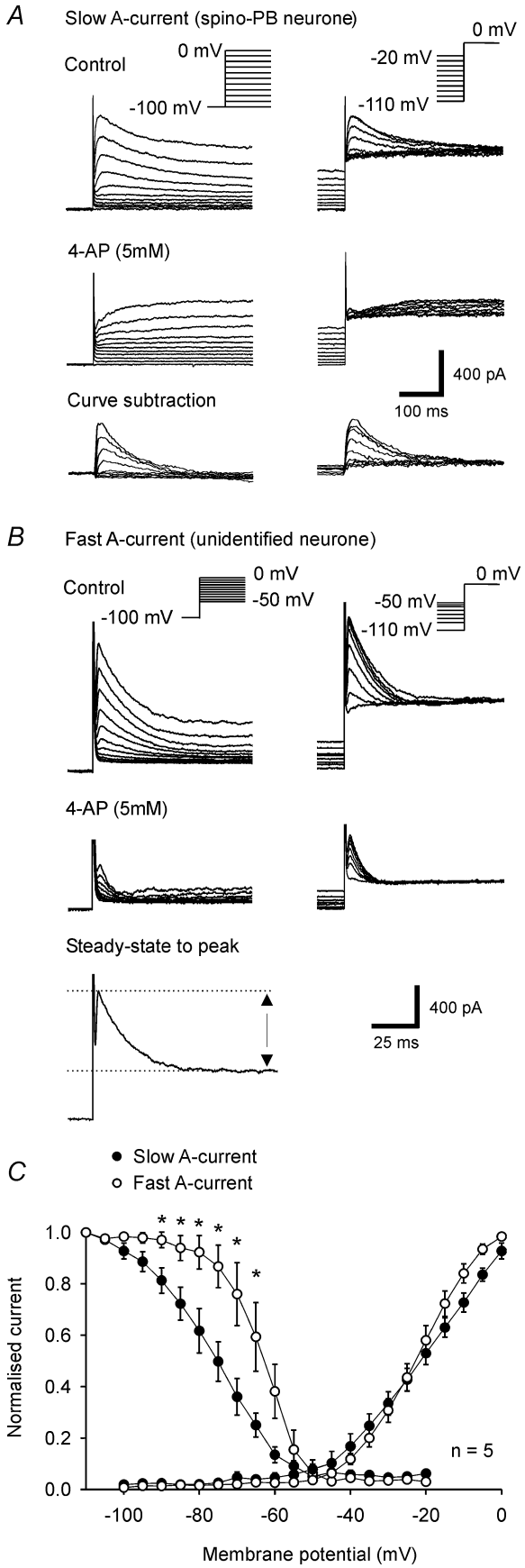

as reflected by the smaller difference between resting membrane potential and action potential threshold (Table 2). Projection neurones had significantly larger membrane capacitances and lower membrane resistances than unidentified neurones, consistent with their larger somatic size seen in Lucifer yellow-labelled neurones (Tables 1 and 2).

When neurones were grouped not according to projection but according to firing patterns (results summarized in Table 3), it became evident that burst and gap firing neurones largely differ in their membrane properties. Most prominent was the high membrane excitability of burst firing neurones. Differences in excitability and other properties were also found between the gap and burst firing neurones and neurones exhibiting the tonic and delayed firing patterns that are the patterns most frequently encountered in unidentified neurones.

Primary afferent input from the dorsal root

In 143 neurones, we tested if electrical stimulation of Aδ- and/or C-fibres in the dorsal root evoked excitatory postsynaptic currents (EPSCs). This was significantly ($P < 0.05$) more often the case in projection neurones (81% of the tested spino-parabrachial neurones, 87% of the tested spino-PAG neurones) than in unidentified neurones (69% of the tested unidentified neurones). The results are summarized in Table 4. Most prominent was the fact that few of the unidentified neurones but one-third of the spino-parabrachial neurones and almost two-thirds of the spino-PAG neurones received monosynaptic

Figure 6. Activation and steady-state inactivation of the two A-currents

A and *B,* activation was assessed by applying graded depolarizing voltage steps (−100 to 0 mV) from a holding potential of −100 mV (left column). Inactivation was evaluated by depolarizing voltage steps to 0 mV applied from different holding potentials (−110 to −20 mV, right column). *A,* the slow A-current was abolished by 4-AP (5 mM). The remaining delayed K^+ current was large in comparison to the A-current. Therefore, the amplitude of the slow A-current was measured after subtracting the curves under 4-AP from the control curves. Insets, voltage step protocols. *B,* the fast A-current was only partially suppressed by 4-AP (5 mM). Therefore, the amplitude of the fast A-current was measured by subtracting the steady-state current at the end of the 200 ms voltage pulse from the maximal current evoked by the voltage step. Insets, voltage step protocols. *C,* activation and steady-state inactivation of both A-currents were voltage-dependent. Currents were normalized to the current evoked by a voltage step from −110 to 0 mV. Inactivation was significantly larger ($P < 0.05$) for the slow A-current than for the fast A-current at the voltages indicated by a star. All experiments were conducted in TTX (0.5 μM).

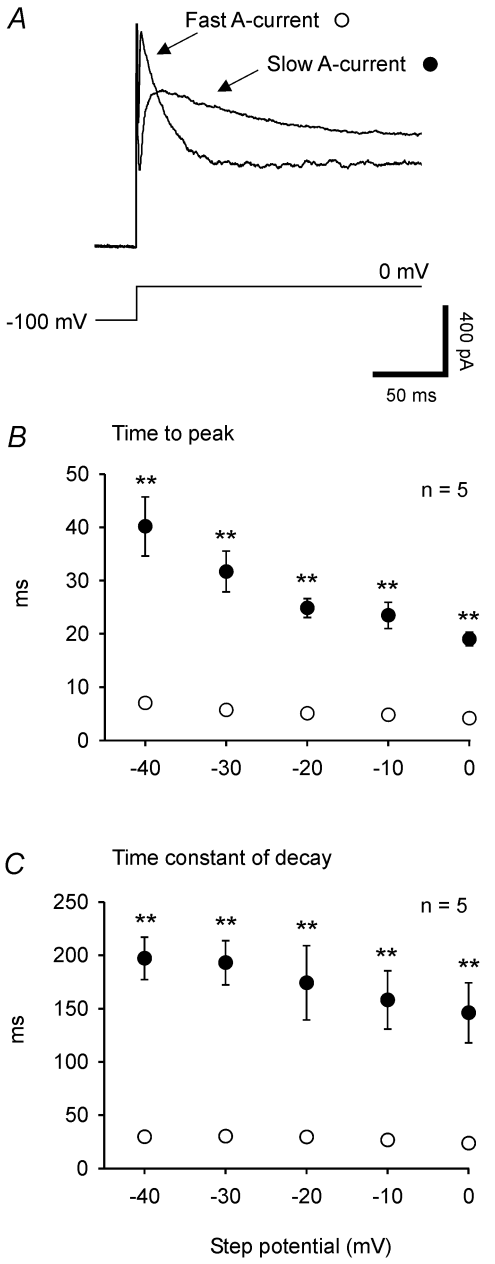

Figure 7. Activation and inactivation kinetics of the two A-currents

A, superposition of exemplary traces of the slow and the fast A-current evoked by a voltage step from −100 to 0 mV illustrates the differences in their kinetics of activation and inactivation. *B,* the time to peak was measured from the onset of the voltage pulse (−100 mV to the value indicated in the graph) to the maximum of the A-current. *C,* the time constant of decay was evaluated by a monoexponential fit to the decay phase of the current. For measuring the time to peak and the time constant of decay of the slow A-current, the subtracted curve was used (see Fig. 6*A*). Both the time to peak and the time constant of decay were voltage-dependent and significantly shorter in the fast A-current than in the slow A-current (**$P < 0.01$). Voltage dependence appears to be larger for the slow A-current because of scaling effects but was in reality similar for the two A-currents. Experiments were conducted in TTX (0.5 μM).

input from primary afferent C-fibres ($P < 0.01$ for comparison of unidentified neurones with spino-PAG neurones). Spino-PAG neurones seldom received input from primary afferent Aδ-fibres, and if they did, the EPSCs were significantly smaller in amplitude than those evoked by stimulation of C-fibres ($P < 0.01$, Table 4).

Discussion

The main results of this study are that lamina I neurones with a projection to the parabrachial area or to the PAG differ from unidentified lamina I neurones in firing patterns, membrane properties and primary afferent input.

The spino-parabrachial and spino-PAG pathways are thought to be involved in autonomic and emotional responses to painful stimuli and in the ascending part of an antinociceptive feedback loop (Bester *et al.* 2000; Millan, 2002; Keay & Bandler, 2002). In contrast, the spino-thalamic pathway is supposed to subserve discriminative evaluation of painful stimuli (Gauriau & Bernard, 2002). However, most lamina I neurones projecting to the thalamus or to the PAG have collaterals to the parabrachial area (Hylden *et al.* 1989; Spike *et al.* 2003). Similarly, the populations of lamina I neurones projecting to the parabrachial area and the caudal ventrolateral medulla seem to largely overlap (Spike *et al.* 2003) and all these pathways to supraspinal targets share a similar proportion of NK1 receptor expressing neurones (Marshall *et al.* 1996; Todd *et al.* 2000). It is therefore tempting to hypothesize that a uniform population of lamina I nociceptive projection neurones sends its axon collaterals to several supraspinal targets where their information can be used either for discriminative or more integrative purposes. However, we found two very distinct groups of projection neurones: the gap firing and the burst firing neurones. Burst firing neurones had easily excitable membranes, narrow action potentials, pronounced afterdepolarizations and frequent monosynaptic input from primary afferent C-fibres and were found preferentially among the spino-PAG neurones. Gap firing neurones had less excitable membranes and broad action potentials due to a hump in the falling phase of the action potential. Gap firing neurones were preferentially encountered among the spino-parabrachial neurones but also in about half of the spino-PAG neurones. Burst firing neurones seemed to be a more specific input to the PAG. As most lamina I spino-PAG neurones have collaterals to the parabrachial area, they constitute a subgroup of about one-third of the spino-parabrachial population. Nevertheless, they

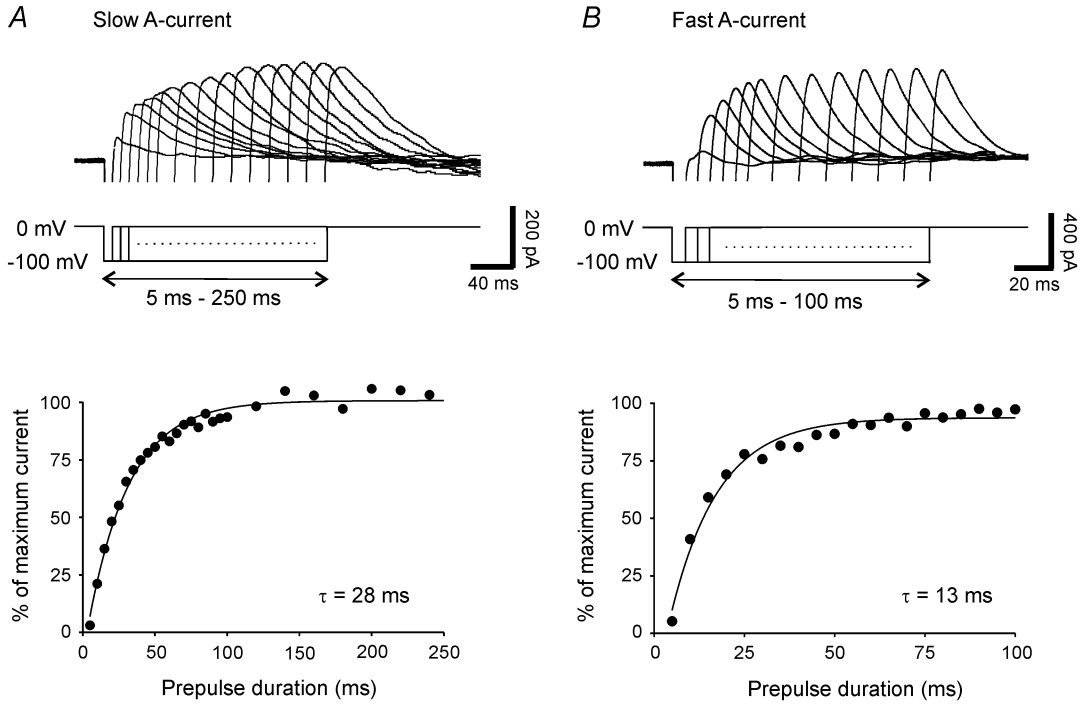

Figure 8. Recovery from steady-state inactivation of the two A-currents
Recovery from steady-state inactivation of the slow A-current (*A*) and the fast A-current (*B*) followed a monoexponential time course. Representative examples are shown. Top traces, recovery from inactivation was assessed by first inactivating the A-current completely at 0 mV, then applying a hyperpolarizing prepulse to −100 mV of varying duration (5–250 ms) before stepping back to 0 mV. Experiments were conducted in TTX (0.5 μM).

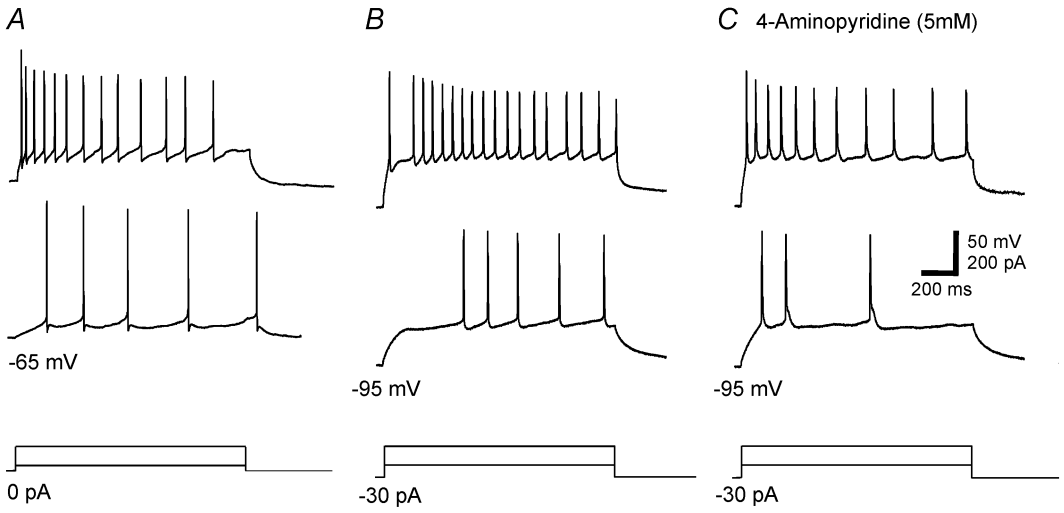

Figure 9. Voltage dependence and sensitivity to 4-AP of the gap firing pattern
A representative example of a gap firing neurone is shown. *A,* when depolarizing current was injected from a holding potential that was more positive than about −75 mV, the neurone showed a tonic firing pattern. *B,* gap firing was unmasked by holding the neurone at a more hyperpolarized potential before injecting depolarizing current to elicit the firing pattern. *C,* during bath application of 4-AP (5 mM), a tonic firing pattern was generated even from a hyperpolarized holding potential. Bottom traces: injected currents, superimposed.

have been shown to differ from other spino-parabrachial neurones, e.g. by exhibiting weaker immunoreactivity for the NK1 receptor than other lamina I projection neurones (Spike *et al.* 2003). Together with our finding that spino-PAG neurones exhibit firing patterns and membrane properties that set them apart from the average of spino-parabrachial neurones, it seems that the spino-PAG neurones may represent a distinct subclass of lamina I projection neurones. The functional significance of these two types of lamina I projection neurones remains to be elucidated. We have recently shown that they express synaptic long-term potentiation in response to different patterns of primary afferent stimulation (Ikeda *et al.* 2003 and authors' unpublished observations). Firing patterns may also be related to the physiological type of the neurone, as suggested by Han *et al.* (1998) for unidentified lamina I neurones. Nociceptive-specific, polymodal nociceptive and thermoreceptive-specific cells are all encountered among lamina I projection neurones in the cat (Craig *et al.* 2001). About 80% of the spino-parabrachial neurones in rat and cat are nociceptive-specific (Hylden *et al.* 1985; Light *et al.* 1993; Bester *et al.* 2000), and 75% of the spino-parabrachial neurones in the present study were of the gap firing type. *In vivo* studies will be needed to investigate if there is a correlation between firing pattern and responses to natural stimulation in lamina I projection neurones.

The PAG is functionally organized in longitudinal columns. Lamina I sends projections to both the lateral PAG that mediates flight behaviour in response to escapable painful stimuli and the ventrolateral PAG that mediates passive behaviour in response to inescapable painful stimuli (Keay & Bandler, 2002). Unexpectedly, we found that the proportion of bursting to gap firing spino-PAG neurones depended on the rostrocaudal position of the injection site. Some functional organization in the rostrocaudal axis has been proposed for the lateral PAG, where the caudal and intermediate portions seem to be responsible for flight and confrontational defence, respectively (Bandler & Shipley, 1994). We do not know if the firing patterns of spino-PAG neurones relate to these functional aspects.

In vivo single-cell recordings have shown lamina I spino-parabrachial neurones to be nociceptive, mostly nociceptive-specific in the rat (Bester *et al.* 2000) and the cat (Hylden *et al.* 1985; Light *et al.* 1993), and to receive convergent input from primary afferent Aδ- and C-fibres

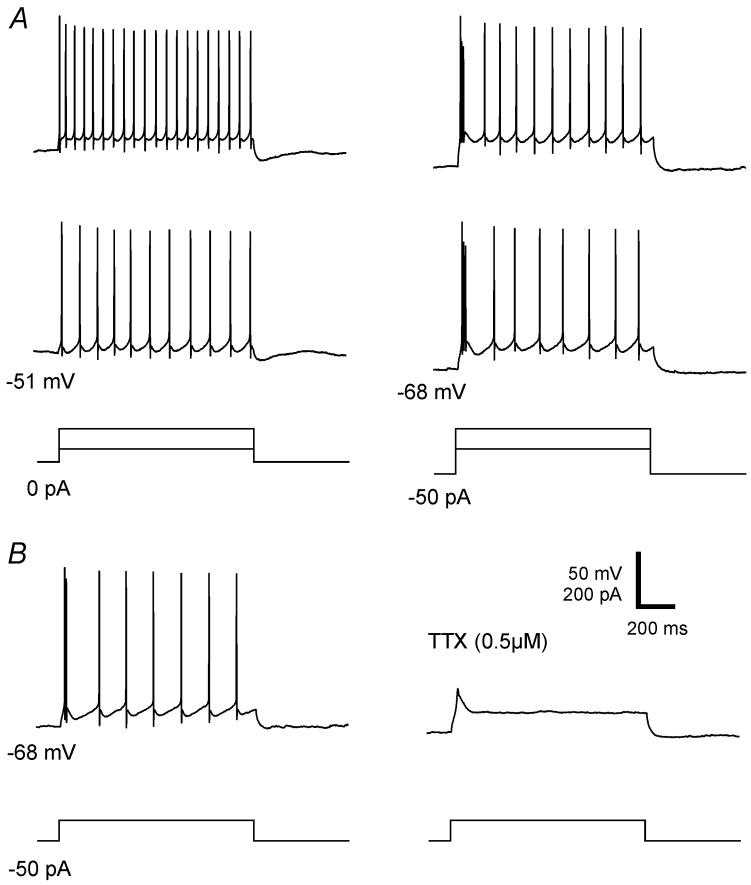

Figure 10. Properties of the bursting firing pattern
A, voltage-dependence of the bursting firing pattern. When the neurone was held at a potential more positive than −60 mV, it showed a tonic firing pattern (left column). From a more hyperpolarized holding potential, the characteristic bursting pattern was evoked (right column). *B,* injection of depolarizing current from a holding potential of −68 mV evoked the bursting firing pattern. When the action potentials were abolished by TTX (0.5 μM), the underlying slow depolarizing wave became evident. *A* and *B,* bottom traces: injected currents, superimposed.

in the rat (Bester *et al.* 2000). In any spinal slice preparation, it is likely that part of the primary afferent input is lost because of damage to some afferent fibres during the slicing process. We found convergent input from Aδ- and C-fibres in 45% of the spino-parabrachial neurones that received input from the segmental dorsal root. Lamina I neurones with a projection to the midbrain (PAG and surrounding structures) have been reported to be mainly nociceptive-specific and to receive primary afferent input from Aδ-fibres in 97% and C-fibres in 20% *in vivo* (Hylden *et al.* 1986). We studied neurones with a projection to the PAG and found input from C-fibres in 94% and input from Aδ-fibres in 25% of the neurones receiving input from the segmental dorsal root. Most prominent, however, was the high incidence of monosynaptic input from primary afferent C-fibres to our population of projection neurones. This and their high membrane excitability might render them especially susceptible for sensitization by nociceptive stimuli.

Unidentified lamina I neurones were different from the projection neurones in almost every aspect investigated in the present study. Most of our unidentified neurones probably were propriospinal neurones. It has been estimated that only 5–10% of lamina I neurones have a supraspinal projection (Bice & Beal, 1997*a*; Bice & Beal, 1997*b*; Spike *et al.* 2003). The chance to record from a projection neurone without the aid of retrograde labelling is therefore low. In our sample, 8% of the unidentified neurones showed the gap or bursting firing pattern typical of projection neurones, suggesting that some projection neurones were indeed recorded by chance.

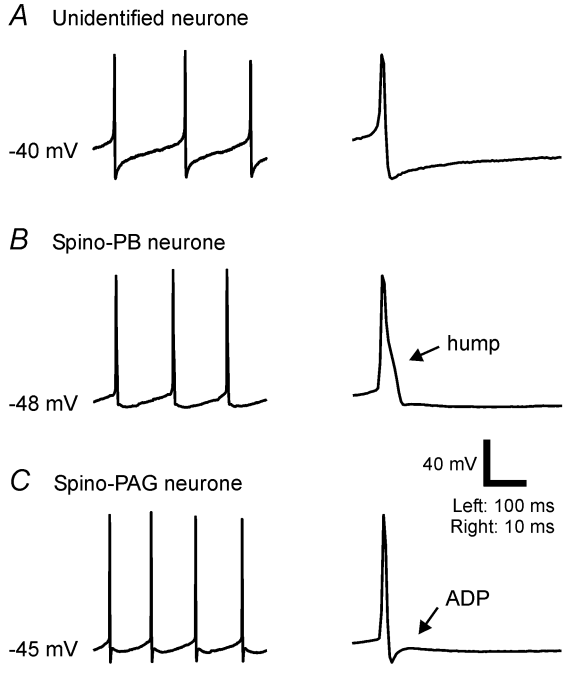

Figure 11. Different shapes of the action potential and its afterpotentials in lamina I unidentified and projection neurones
Representative traces are shown. *A,* in unidentified neurones, action potentials were followed by marked afterhyperpolarizations that could be monophasic as shown here or polyphasic as described elsewhere (Ruscheweyh & Sandkühler, 2002). *B,* spino-parabrachial neurones often exhibited a hump in the falling phase of the action potential. *C,* spino-PAG neurones typically showed action potentials followed by pronounced afterdepolarizations.

The distribution of firing patterns and membrane properties of unidentified lamina I neurones reported here compares mostly well to what we found previously (Ruscheweyh & Sandkühler, 2002). A study on unidentified lamina I neurones in parasagittal spinal cord slices from adult rats revealed similar firing patterns but reported a larger proportion of single spiking *versus* tonic firing neurones (Prescott & De Koninck, 2002). This could be due to the slicing technique, the slicing plane or the age of the animals. Lamina I neurones are known to have large rostrocaudal dendritic arbors (Lima & Coimbra, 1986) that may be damaged by the transverse slicing technique. This might cause a selection bias or modify membrane properties. However, the infrared video contrast microscopy used here allowed us to record from neurones as deep as 100 μm from the surface in 500 μm thick slices, making it quite unlikely that a large proportion of any particular type of neurone was selectively destroyed or damaged. On the other hand, in the study of Prescott & De Koninck (2002), Lucifer yellow was routinely included in the intracellular solution, and this may modify membrane properties (Higure *et al.* 2003). In support of this explanation, in our sample of Lucifer yellow-filled unidentified neurones, 55% of 11 neurones showed the single spike firing pattern, while this was the case only for 9% of the 65 neurones recorded without Lucifer yellow ($P < 0.01$). Overall resting membrane potentials were more negative in the present than in our previous study. We attribute that to an improved recording technique yielding better seals. Membrane resistances were much higher in the present study. This is due to the modified analysis of passive membrane properties as described in Methods.

Intracellular labelling

In rat and cat, lamina I neurones have been morphologically classified into the fusiform, multipolar, pyramidal and flattened subtypes (Lima & Coimbra, 1986; Galhardo & Lima, 1999). It has been reported that in the rat, lamina I spino-parabrachial neurones are

Table 2. Passive and active membrane properties of lamina I unidentified and projection neurones

	Unidentified neurones (UN)	Spino-parabrachial neurones (PB)	Spino-PAG neurones (PAG)
	($n = 64$–66)	($n = 91$–96)	($n = 67$–82)
Resting membrane potential (RMP, mV)	-63 ± 1 **PAG	-63 ± 1 **PAG	-59 ± 1 **UN,**PB
Action potential threshold (mV)	-37 ± 1 **PB,**PAG	-44 ± 1 **UN	-43 ± 1 **UN
Action potential threshold − RMP (mV)	27 ± 1 **PB, **PAG	20 ± 1 **UN	16 ± 1 **UN
Action potential width at base (ms)	2.1 ± 0.1 **PB, **PAG	3.1 ± 0.1 **UN, **PAG	2.4 ± 0.1 **UN, **PB
Afterdepolarization amplitude (mV)	1.4 ± 0.6 **PB, **PAG	2.9 ± 0.4 **UN, **PAG	9.4 ± 0.8 **UN, **PB
	($n = 57$)	($n = 27$)	($n = 25$)
Membrane resistance (MΩ)	1534 ± 57 **PB, **PAG	1009 ± 76 **UN	839 ± 25 **UN
Membrane capacitance (pF)	37 ± 2 **PB,**PAG	81 ± 5 **UN	77 ± 5 **UN

Statistical significance was assessed by one-way ANOVA that yielded $P < 0.001$ for every row. **, $P < 0.01$ in the posthoc test, followed by the abbreviation of the group the comparison was made with. *n*, number of observations.

mostly fusiform while spino-PAG neurones are mostly pyramidal (Lima & Coimbra, 1989). This view has recently been challenged by Spike *et al.* (2003) who found that in the rat, both spino-parabrachial and spino-PAG neurones are about evenly distributed among fusiform, pyramidal and multipolar (including flattened) neurones. Unequivocal morphological classification of lamina I neurones according to Lima and Coimbra (Lima & Coimbra, 1986; Galhardo & Lima, 1999) is not possible in the transverse plane. We have therefore abstained from classifying the neurones of the present study by their morphology. In our transverse spinal cord slice preparation, a majority of projection neurones had prominent mediolateral dendrites, thus probably belonging to the pyramidal or flattened classes. In contrast, many unidentified neurones had a more ventral orientation of their dendritic trees, probably corresponding to the multipolar or fusiform type. Similar to our results, *in vivo* intracellular labelling of lamina I spino-parabrachial neurones in the cat produced mainly neurones with dendrites confined to lamina I and a considerable mediolateral extent (Light *et al.* 1993). In many of our projection neurones, long axons were seen that coursed laterally, often reaching the lateral edge of the dorsal horn, similar to what has been reported in the cat (Light *et al.* 1993). Spino-parabrachial neurones send their ascending axons through the dorsolateral funiculus but often have collaterals in the dorsal horn (Hylden *et al.* 1989; Light *et al.* 1993). We do not know if the axons seen here were ascending or segmental collaterals.

Firing patterns and responses to natural stimulation of the skin have been reported to be related to the morphological type of lamina I neurones in the rat (Prescott & De Koninck, 2002) and the cat (Han *et al.* 1998), respectively. These results have been obtained in unidentified lamina I neurones. Further investigations will be needed to determine if these findings extend to projection neurones.

The gap and delayed firing patterns and the underlying A-currents

The gap firing pattern is not a common one in the nervous system but it has been described, e.g. in the superior colliculus (Saito & Isa, 2000) and in vagal motoneurones (Yarom *et al.* 1985). In olivocochlear neurones, both the delayed and the gap firing pattern occur. As reported here for the spinal dorsal horn, they belong to two groups of neurones with different functions and projections (Fujino *et al.* 1997). Similar to our results, in olivocochlear neurones the A-current responsible for the gap firing pattern had slower kinetics than the A-current belonging to the delayed firing pattern. Apparently, the slow activation of the A-current in gap firing neurones allows for just one action potential to occur before the gap at the beginning of a depolarizing current pulse. The D-current is another voltage-dependent K^+ current with slow kinetics (Storm, 1988). However, it is highly sensitive to 4-AP and usually completely blocked by 30–100 μM, which was not the case for the slow A-current described here.

The mean resting membrane potentials of gap and delayed firing neurones (−63 and −68 mV, respectively) fall into the steep regions of their respective inactivation curves (Fig. 6*C*). Thus, small variations of the resting membrane potential may have large impacts on A-current-modulated features of the neurone, among them action potential width, firing frequency and firing patterns (Rogawski, 1985). Excitatory postsynaptic potentials (EPSPs), especially large ones, are shortened in neurones expressing A-currents, which may be important for temporal summation of synaptic inputs (Cassell & McLachlan, 1986). As a general rule, A-currents reduce the

Table 3. Passive and active membrane properties of lamina I unidentified and projection neurones classified according to their firing patterns

	Gap firing (G)	Bursting (B)	Tonic firing (T)	Delayed firing (D)	Initial burst (IB)	Single spike (S)	Phasic burst (PB)
	(n = 98–104)	(n = 26–37)	(n = 37–38)	(n = 10–11)	(n = 3)	(n = 6–7)	(n = 18–20)
Resting membrane potential (RMP; mV)	−63 ± 1 **B	− 57 ± 1 **D, **G	−62 ± 1	−68 ± 2 **B	−61 ± 4	−66 ± 3	−63 ± 1
Action potential threshold (mV)	−42 ± 1 **D, **B	− 48 ± 1 **D, **G, **PB, **T	−39 ± 1 **B	−29 ± 3 **G, **B	−38 ± 2	−40 ± 3	−41 ± 2 **B
Action potential threshold – RMP (mV)	21 ± 1 **D, **B	9 ± 1 **D, **G, **PB, **T	23 ± 2 **D, **B	39 ± 4 **G, **B, **PB, **T	23 ± 6	25 ± 5	22 ± 2 **D, **B
Action potential width at base (ms)	2.9 ± 0.1 **B, **S, **T	2.1 ± 0.1 **G	2.3 ± 0.1 **G	2.3 ± 0.2	2.1 ± 0.1	1.7 ± 0.2 **G	2.4 ± 0.2
Afterdepolarization amplitude (mV)	4.2 ± 0.5 **D, **B, **PB	12.9 ± 1.0 **D, **G, **PB, **S, **T	3.1 ± 0.9 **B	0 ± 0 **G, **B	0 ± 0	0 ± 0 **B	0.9 ± 0.5 **G, **B
	(n = 37)	(n = 12)	(n = 22)	(n = 10)	(n = 3)	(n = 6)	(n = 8)
Membrane resistance (MΩ)	996 ± 81 **T	604 ± 63 **D, **S, **T	1709 ± 207 **G, **B	1136 ± 98 **B	1331 ± 35	1319 ± 122 **B	1704 ± 355
Membrane capacitance (pF)	82 ± 5 **D, **PB, **S, **T	72 ± 6 **D, *PB, **T	35 ± 3 **G, **B	33 ± 3 **G, **B	51 ± 8	38 ± 2 **G	37 ± 4 **G, *B

Statistical significance was assessed by one-way ANOVA that yielded $P < 0.001$ for every row. *$P < 0.05$, **$P < 0.01$ in the *post hoc* test, followed by the abbreviation of the group the comparison was made with. n, number of observations.

excitability of neurones (Banks *et al.* 1996), especially when the membrane is already hyperpolarized by other factors such as inhibitory synaptic input. One might call this a potentiation of inhibition and hypothesize that, in the presence of intact segmental and descending inhibition, this mechanism protects gap firing projection neurones from sensitization.

The bursting firing pattern

The bursting firing pattern has not previously been described in the spinal dorsal horn. However, rebound spikes in response to release from hyperpolarizing current may have a similar mechanism and have been reported in a few dorsal horn neurones (Jiang *et al.* 1995; Ruscheweyh & Sandkühler, 2002). In the brain, the bursting firing pattern is more common and has been attributed to low threshold voltage-dependent Ca^{2+} channels (T-current) (Destexhe *et al.* 1998), high threshold voltage-dependent Ca^{2+} channels (Jung *et al.* 2001) or TTX-sensitive persistent Na^{+} channels (Azouz *et al.* 1996). In the present study, the slow depolarizing wave on which the burst rides persisted in TTX (Fig. 10*B*). The underlying current seemed to be a Ca^{2+} current as it was partially blocked by Ni^{2+} and Cd^{2+}. Even if full characterization of the current was not possible, its low activation threshold (−60 mV) and its inactivation at similar voltages, inferred from the conversion of the firing pattern from bursting to tonic at these voltages (Fig. 10*A*), suggest that it may be a T-current (McRory *et al.* 2001; Perez-Reyes, 2003).

Low-threshold Ca^{2+} channels mediate Ca^{2+} entry during excitatory postsynaptic potentials (EPSPs) and action potentials (Kozlov *et al.* 1999) and increase the neuronal excitability by 'boosting' EPSPs and thus lowering the threshold for action potential generation (Huguenard, 1996). They also increase the EPSP duration, facilitating temporal summation (Williams & Stuart, 1999). In addition, they are able to convert inhibitory signals into excitatory ones by generating postinhibitory rebound spikes, especially when the resting membrane potential is both near the threshold for activation and inactivation as in the present study (Destexhe *et al.* 1998).

In conclusion, we have shown that lamina I unidentified neurones, most of them probably propriospinal, have properties that are fundamentally different from those of lamina I neurones with a supraspinal projection. The projection neurones, however, are also not a homogeneous group. The spino-PAG neurones seem to constitute a small but distinctive subgroup of the lamina I projection neurones with respect to firing patterns and membrane properties.

Table 4. Primary afferent input to lamina I unidentified and projection neurones

	Unidentified neurones ($n = 43$)	Spino-parabrachial neurones ($n = 22$)	Spino-PAG neurones ($n = 47$)
Aδ-fibre monosynaptic	4 (14%)	2 (9%)	1 (2%)
Aδ-fibre polysynaptic	22 (51%)	10 (45%)	11 (23%)
C-fibre monosynaptic	6 (14%)	7 (32%)	27 (58%)
C-fibre polysynaptic	27 (63%)	13 (59%)	17 (36%)
Convergent A- and C-fibre	16 (37%)	10 (45%)	9 (19%)
Peak amplitude of Aδ-fibre input (pA)	207 ± 28 ($n = 26$)	241 ± 47 ($n = 12$)	107 ± 24 ($n = 7$)
Peak amplitude of C-fibre input (pA)	238 ± 40 ($n = 30$)	471 ± 94 ($n = 19$)	363 ± 56 ($n = 38$)

n, number of neurones with input from primary afferents. For numbers of tested cells, refer to the text.

References

Azouz R, Jensen MS & Yaari Y (1996). Ionic basis of spike after-depolarization and burst generation in adult rat hippocampal CA1 pyramidal cells. *J Physiol* **492**, 211–223.

Bandler R & Shipley MT (1994). Columnar organization in the midbrain periaqueductal gray: modules for emotional expression? *Trends Neurosci* **17**, 379–389.

Banks MI, Haberly LB & Jackson MB (1996). Layer-specific properties of the transient K^+ current (I_A) in piriform cortex. *J Neurosci* **16**, 3862–3876.

Bester H, Chapman V, Besson JM & Bernard JF (2000). Physiological properties of the lamina I spinoparabrachial neurons in the rat. *J Neurophysiol* **83**, 2239–2259.

Bice TN & Beal JA (1997*a*). Quantitative and neurogenic analysis of neurons with supraspinal projections in the superficial dorsal horn of the rat lumbar spinal cord. *J Comp Neurol* **388**, 565–574.

Bice TN & Beal JA (1997*b*). Quantitative and neurogenic analysis of the total population and subpopulations of neurons defined by axon projection in the superficial dorsal horn of the rat lumbar spinal cord. *J Comp Neurol* **388**, 550–564.

Cassell JF & McLachlan EM (1986). The effect of a transient outward current (I_A) on synaptic potentials in sympathetic ganglion cells of the guinea pig. *J Physiol* **374**, 273–288.

Cervero F & Tattersall JE (1987). Somatic and visceral inputs to the thoracic spinal cord of the cat: marginal zone (lamina I) of the dorsal horn. *J Physiol* **388**, 383–395.

Chen J & Sandkühler J (2000). Induction of homosynaptic long-term depression at spinal synapses of sensory Aδ-fibers requires activation of metabotropic glutamate receptors. *Neuroscience* **98**, 141–148.

Christensen BN & Perl ER (1970). Spinal neurons specifically excited by noxious or thermal stimuli: marginal zone of dorsal horn. *J Neurophysiol* **33**, 293–307.

Craig AD, Krout K & Andrew D (2001). Quantitative response characteristics of thermoreceptive and nociceptive lamina I spinothalamic neurons in the cat. *J Neurophysiol* **86**, 1459–1480.

Destexhe A, Neubig M, Ulrich D & Huguenard J (1998). Dendritic low-threshold calcium currents in thalamic relay cells. *J Neurosci* **18**, 3574–3588.

Ding Y, Takada M, Shigemoto R & Mizuno N (1995). Spinoparabrachial tract neurons showing substance P receptor-like immunoreactivity in the lumbar spinal cord of the rat. *Brain Res* **674**, 336–340.

Fujino K, Koyano K & Ohmori H (1997). Lateral and medial olivocochlear neurons have distinct electrophysiological properties in the rat brain slice. *J Neurophysiol* **77**, 2788–2804.

Galhardo V & Lima D (1999). Structural characterization of marginal (lamina I) spinal cord neurons in the cat: a Golgi study. *J Comp Neurol* **414**, 315–333.

Gauriau C & Bernard JF (2002). Pain pathways and parabrachial circuits in the rat. *Exp Physiol* **87**, 251–258.

Han ZS, Zhang ET & Craig AD (1998). Nociceptive and thermoreceptive lamina I neurons are anatomically distinct. *Nat Neurosci* **1**, 218–225.

Higure Y, Katayama Y, Takeuchi K, Ohtubo Y & Yoshii K (2003). Lucifer Yellow slows voltage-gated Na^+ current inactivation in a light-dependent manner in mice. *J Physiol* **550**, 159–167.

Huguenard JR (1996). Low-threshold calcium currents in central nervous system neurons. *Annu Rev Physiol* **58**, 329–348.

Hylden JL, Anton F & Nahin RL (1989). Spinal lamina I projection neurons in the rat: collateral innervation of parabrachial area and thalamus. *Neuroscience* **28**, 27–37.

Hylden JL, Hayashi H, Bennett GJ & Dubner R (1985). Spinal lamina I neurons projecting to the parabrachial area of the cat midbrain. *Brain Res* **336**, 195–198.

Hylden JL, Hayashi H, Dubner R & Bennett GJ (1986). Physiology and morphology of the lamina I spinomesencephalic projection. *J Comp Neurol* **247**, 505–515.

Ikeda H, Heinke B, Ruscheweyh R & Sandkühler J (2003). Synaptic plasticity in spinal lamina I projection neurons that mediate hyperalgesia. *Science* **299**, 1237–1240.

Jiang MC, Cleland CL & Gebhart GF (1995). Intrinsic properties of deep dorsal horn neurons in the L_6-S_1 spinal cord of the intact rat. *J Neurophysiol* **74**, 1819–1827.

Jung HY, Staff NP & Spruston N (2001). Action potential bursting in subicular pyramidal neurons is driven by a calcium tail current. *J Neurosci* **21**, 3312–3321.

Keay KA & Bandler R (2002). Distinct central representations of inescapable and escapable pain: observations and speculation. *Exp Physiol* **87**, 275–279.

Khasabov SG, Rogers SD, Ghilardi JR, Peters CM, Mantyh PW & Simone DA (2002). Spinal neurons that possess the substance P receptor are required for the development of central sensitization. *J Neurosci* **22**, 9086–9098.

Kozlov AS, McKenna F, Lee JH, Cribbs LL, Perez-Reyes E, Feltz A & Lambert RC (1999). Distinct kinetics of cloned T-type Ca^{2+} channels lead to differential Ca^{2+} entry and frequency-dependence during mock action potentials. *Eur J Neurosci* **11**, 4149–4158.

Light AR, Sedivec MJ, Casale EJ & Jones SL (1993). Physiological and morphological characteristics of spinal neurons projecting to the parabrachial region of the cat. *Somatosens Mot Res* **10**, 309–325.

Lima D & Coimbra A (1986). A Golgi study of the neuronal population of the marginal zone (lamina I) of the rat spinal cord. *J Comp Neurol* **244**, 53–71.

Lima D & Coimbra A (1989). Morphological types of spinomesencephalic neurons in the marginal zone (lamina I) of the rat spinal cord, as shown after retrograde labelling with cholera toxin subunit B. *J Comp Neurol* **279**, 327–339.

Mantyh PW, Rogers SD, Honore P, Allen BJ, Ghilardi JR, Li J, Daughters RS, Lappi DA, Wiley RG & Simone DA (1997). Inhibition of hyperalgesia by ablation of lamina I spinal neurons expressing the substance P receptor. *Science* **278**, 275–279.

Marshall GE, Shehab SA, Spike RC & Todd AJ (1996). Neurokinin-1 receptors on lumbar spinothalamic neurons in the rat. *Neuroscience* **72**, 255–263.

McRory JE, Santi CM, Hamming KS, Mezeyova J, Sutton KG, Baillie DL, Stea A & Snutch TP (2001). Molecular and functional characterization of a family of rat brain T-type calcium channels. *J Biol Chem* **276**, 3999–4011.

Millan MJ (2002). Descending control of pain. *Prog Neurobiol* **66**, 355–474.

Nichols ML, Allen BJ, Rogers SD, Ghilardi JR, Honore P, Luger NM, Finke MP, Li J, Lappi DA, Simone DA & Mantyh PW (1999). Transmission of chronic nociception by spinal neurons expressing the substance P receptor. *Science* **286**, 1558–1561.

Perez-Reyes E (2003). Molecular physiology of low-voltage-activated T-type calcium channels. *Physiol Rev* **83**, 117–161.

Prescott SA & De Koninck Y (2002). Four cell types with distinctive membrane properties and morphologies in lamina I of the spinal dorsal horn of the adult rat. *J Physiol* **539**, 817–836.

Rogawski MA (1985). The A-current: how ubiquitous a feature of excitable cells is it? *Trends Neurosci* **8**, 214–219.

Ruscheweyh R & Sandkühler J (2002). Lamina-specific membrane and discharge properties of rat spinal dorsal horn neurones in vitro. *J Physiol* **541**, 231–244.

Saito Y & Isa T (2000). Voltage-gated transient outward currents in neurons with different firing patterns in rat superior colliculus. *J Physiol* **528**, 91–105.

Sandkühler J (2000). Learning and memory in pain pathways. *Pain* **88**, 113–118.

Spike RC, Puskár Z, Andrew D & Todd AJ (2003). A quantitative and morphological study of projection neurons in lamina I of the rat lumbar spinal cord. *Eur J Neurosci* **18**, 2433–2448.

Storm JF (1988). Temporal integration by a slowly inactivating K^+ current in hippocampal neurons. *Nature* **336**, 379–381.

Suzuki R, Morcuende S, Webber M, Hunt SP & Dickenson AH (2002). Superficial NK1-expressing neurons control spinal excitability through activation of descending pathways. *Nat Neurosci* **5**, 1319–1326.

Swanson LW (1992). *Brain Maps: Structure of the Rat Brain.* Elsevier, Amsterdam.

Todd AJ, McGill MM & Shehab SA (2000). Neurokinin 1 receptor expression by neurons in laminae I, III and IV of the rat spinal dorsal horn that project to the brainstem. *Eur J Neurosci* **12**, 689–700.

Williams SR & Stuart GJ (1999). Mechanisms and consequences of action potential burst firing in rat neocortical pyramidal neurons. *J Physiol* **521**, 467–482.

Willis WD & Coggeshall RE (1991). *Sensory Mechanisms of the Spinal Cord*. Plenum Press, New York.

Yarom Y, Sugimori M & Llinas R (1985). Ionic currents and firing patterns of mammalian vagal motoneurons *in vitro*. *Neuroscience* **16**, 719–737.

Acknowledgements

The authors wish to thank L. Forsthuber for technical assistance with the two-dimensional reconstruction of Lucifer yellow-labelled neurones. This work was supported by grant P15542 from the Fonds zur Förderung der wissenschaftlichen Forschung (Austria) and by the Medizinisch-Wissenschaftlicher Fonds des Bürgermeisters der Bundeshauptstadt Wien. H.I. was partially supported by the Japan Society for the Promotion of Science.

Author's present address

H. Ikeda: Department of Human and Artificial Intelligence Systems, Fukui University, Fukui, Japan.